Anomalous current transport in Au/low-doped n-GaAs Schottky barrier diodes at low temperatures

S. Hardikar[1], **M.K. Hudait**[1,2], **P. Modak**[1], **S.B. Krupanidhi**[2,*], **N. Padha**[3]

[1] Central Research Laboratory, Bharat Electronics Ltd., Bangalore - 560 013, India
[2] Materials Research Center, Indian Institute of Science, Bangalore - 560 012, India
(Fax: +91-80/334-1683, E-mail: sbk@mrc.iisc.ernet.in)
[3] Department of Physics and Electronics, University of Jammu, Jammu - 180 004, India

Abstract. The current–voltage characteristics of Au/low-doped n-GaAs Schottky diodes were determined at various temperatures in the range of 77–300 K. The estimated zero-bias barrier height and the ideality factor assuming thermionic emission (TE) show a temperature dependence of these parameters. While the ideality factor was found to show the T_0 effect, the zero-bias barrier height was found to exhibit two different trends in the temperature ranges of 77–160 K and 160–300 K. The variation in the flat-band barrier height with temperature was found to be $-(4.7 \pm 0.2) \times 10^4$ eVK^{-1}, approximately equal to that of the energy band gap. The value of the Richardson constant, A^{**}, was found to be 0.27 A cm^{-2}K^{-2} after considering the temperature dependence of the barrier height. The estimated value of this constant suggested the possibility of an interfacial oxide between the metal and the semiconductor. Investigations suggested the possibility of a thermionic field-emission-dominated current transport with a higher characteristic energy than that predicted by the theory. The observed variation in the zero-bias barrier height and the ideality factor could be explained in terms of barrier height inhomogenities in the Schottky diode.

PACS: 72.10.-d; 73.30.+y; 73.40.GK

The current transport across a Schottky junction is of interest to materials physicists and device physicists. Schottky barrier diodes (SBD) are widely studied and many attempts have been made to understand their behaviour. The knowledge of the conduction mechanism across the Schottky barrier is essential in order to calculate the Schottky barrier parameters and explain the observed effects. Generally, the SBD parameters are determined over a wide range of temperatures in order to understand the nature of the barrier and the conduction mechanism. Although the thermionic emission (TE) theory is normally used to extract the SBD parameters, there have been reports of certain anomalies at lower temperatures deviating from the theory. The ideality factor and the barrier height determined from the forward-bias current–voltage (I–V) characteristics are found to be a strong function of temperature [1–7]. The ideality factor is found to increase with decreasing temperature. This effect, known as the T_0, effect was first reported by Padovani and Sumner [1] and is widely studied. The zero-bias barrier height as determined from the forward-bias I–V characteristics for the thermionic emission decreases with decreasing temperature. The zero-bias barrier height appears to be lower than the barrier height obtained from the capacitance–voltage (C–V) measurements in the temperature range used for the study. This implies that there is an excess current flow in the diodes than that predicted by the thermionic emission theory. Explanations of the possible origin of such anomalies have been proposed taking into account the interface state density distribution [8, 9], quantum-mechanical tunnelling including the thermionic field emission [2, 10–12] and more recently the lateral distribution of barrier height inhomogenities [5, 13–15]. We have studied the forward-bias I–V characteristics of a Au/n-GaAs Schottky diode in the low temperature range of 77–300 K, with the doping concentration of the n-GaAs well within the domain of the TE theory and found some anomalies. Attempts were made to examine the possible factors contributing to the observed anomalies based on the proposed theories.

1 Experimental

The Schottky diodes were fabricated on epitaxial undoped GaAs film, grown on silicon-doped (2×10^{18} cm^{-3}) n$^+$-GaAs substrates (100) 2° off-oriented towards the ⟨110⟩ direction, using the metal organic chemical vapor deposition (MOCVD) technique, by evaporating gold under vacuum. The back ohmic contact was made using Au−Ge eutectic with an overlayer of gold. The growth procedure used yields an epitaxial film of n-type conductivity with an unintentional doping concentration of the order of 10^{15} cm^{-3} [16].

Room temperature I–V characteristics of the diodes were measured using an automated arrangement consisting of a Keithley source measure unit SMU236, a PC486 and a probe station. Diodes amongst several diodes showing similar I–V characteristics at room temperature were

* To whom all the correspondence should be addressed

mounted and bonded on TO-39 headers. Low-temperature *I–V* characteristics were obtained in the temperature range of 77–300 K using the automated setup mentioned above and a cryostat. The temperature was within ±1 K during the data acquisition.

The carrier concentration of the epitaxial layer, $2.5\times 10^{15}\,\mathrm{cm}^{-3}$, was determined using the reverse-bias *C–V* characteristics at 1 MHz on a HP4194A LCR bridge and was further confirmed by means of electrochemical *C–V* characteristics.

2 Method of analysis

2.1 Forward I–V characteristics

The current density vs. voltage (*J–V*) characteristics of the Schottky diode are plotted as a function of temperature in Fig. 1. The plot exhibits a linear portion over 3–4 decades of magnitude of current density. The diode ideality factor, n, the saturation current density, J_s, and the barrier height, Φ_b were measured by using the TE theory. According to the TE theory the current transport across a Schottky diode is governed by the relation [17]

$$J = A^{**}T^2 \exp\left(-q\Phi_\mathrm{b}/kT\right)\left[\exp\left(qV/nkT\right)\right] \text{ for } V > 3kT/q\,, \tag{1}$$

$$J_\mathrm{s} = A^{**}T^2 \exp\left(-q\Phi_\mathrm{b}/kT\right)\,, \tag{2}$$

where A^{**} is the Richardson constant for GaAs.

The linear portion of the *J–V* characteristics was plotted on a semi-log plot to extract the Schottky diode parameters viz. the ideality factor, n, and the zero-bias barrier height, Φ_b. The value of $A^{**} = 8\,\mathrm{A\,cm^{-2}K^{-2}}$ was used to calculate the value of the zero-bias barrier height.

The ideality factor and the zero-bias barrier height, are plotted as a function of temperature in Fig. 2. The plot shows that the ideality factor exhibits an increasing trend with decreasing temperature, the change being more pronounced below 150 K, whereas the zero-barrier height first increases with decreasing temperature upto 160 K and then decreases. This apparent decrease in the zero-bias barrier height below 160 K is consistent with the observations made by others on different Schottky diodes [3–7]. They found that the zero-bias barrier height decreases with decreasing temperature. The increase in the zero-bias barrier height with decreasing temperature in the 160–300 K range is similar to the variation in the barrier height measured by *C–V* measurements and has not been reported in the literature.

2.1.1 Flat-band barrier height. The barrier height as obtained from the TE theory decreases with decreasing temperature. The barrier height obtained from (1) is called the apparent barrier height or the zero-bias barrier height. The barrier height obtained under flat-band condition is called the flat-band barrier height and is considered the real fundamental quantity. Unlike the case of the zero-bias barrier height, the electric field in the semiconductor is zero under the flat-band conditions. The flat-band barrier height is given by [18].

$$\Phi_\mathrm{b}^\mathrm{f} = n\Phi_\mathrm{b} - (n-1)kT\ln\left(N_\mathrm{C}/N_\mathrm{D}\right)\,, \tag{3}$$

where Φ_b is the zero-bias barrier height, N_C is the density of states in the conduction band, and N_D is the doping concentration in the semiconductor.

The variation in $\Phi_\mathrm{b}^\mathrm{f}$ as a function of temperature is shown in Fig. 3. $\Phi_\mathrm{b}^\mathrm{f}$ increases with decreasing temperature in the 150–300 K range and, anomalously, decreases below 150 K. A linear fit is used to fit the points in the range of 150–300 K in order to determine the slope and the y-axis intercept, which

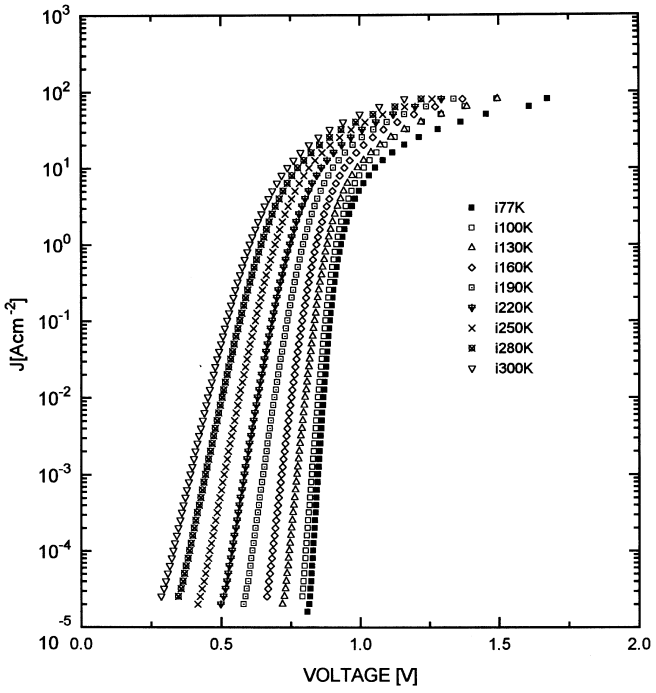

Fig. 1. The current density vs. voltage characteristics of the Au/n-GaAs Schottky diode at various temperatures

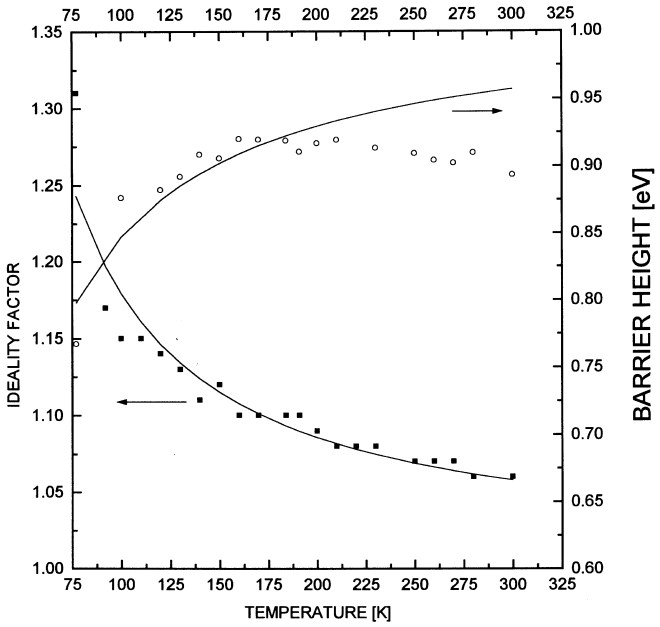

Fig. 2. The variation in the zero-bias barrier height and the ideality factor with temperature, calculated using (1) and (2), for the Au/n-GaAs Schottky diode. The zero-bias barrier height increases with decreasing temperature up to 160 K and then decreases in the 77–160 K range

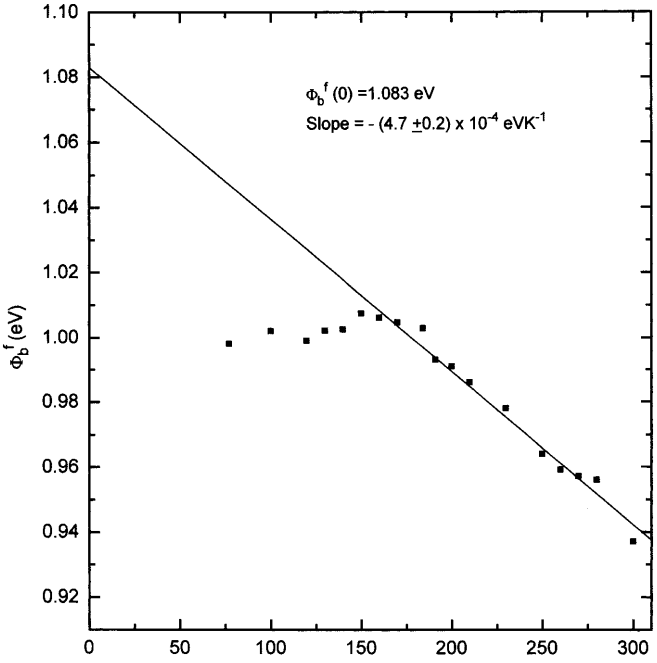

Fig. 3. The flat-band barrier height, calculated using (3), as a function of temperature. The *continuous line* represents the best fit to the points in the 150–300 K range. The slope and the barrier height at 0 K are shown in the figure

give the value of $\mathrm{d}\Phi_\mathrm{b}^\mathrm{f}/\mathrm{d}T$ and the value of barrier height at absolute zero, $\Phi_\mathrm{b}^\mathrm{f}$ (0), respectively. The linear fit yields a slope, $\mathrm{d}\Phi_\mathrm{b}^\mathrm{f}/\mathrm{d}T$ equal to $-(4.7 \pm 0.2) \times 10^{-4}\,\mathrm{eVK}^{-1}$ and an intercept, $\Phi_\mathrm{b}^\mathrm{f}$ (0) equal to 1.083 eV. The value of $\mathrm{d}\Phi_\mathrm{b}^\mathrm{f}/\mathrm{d}T$ is close to the value obtained by assuming that the variation in the value of $\Phi_\mathrm{b}^\mathrm{f}$ (0) is entirely due to the variation in the band gap [3, 19, 20].

2.1.2 Effect of image force. In order to understand the factors influencing the lowering of the barrier height with decreasing temperature, the effect of image-force lowering was first considered. The barrier lowering due to the image-force effect is given by [21].

$$\Delta\Phi_\mathrm{imf} = \left[\left(q^3 N_\mathrm{D}/8\pi^2\varepsilon_\mathrm{s}^3\right)(\Phi_\mathrm{b} - V - \Phi_\mathrm{n} - kT/q)\right]^{1/4}, \qquad (4)$$

where $\Phi_\mathrm{n} = kT/q \ln(N_\mathrm{C}/N_\mathrm{D})$ and V is the applied bias.

The value of $\Delta\Phi_\mathrm{imf}$ found by using (4) is 13.8 meV at 77 K for a Φ_b of 0.89 V and a typical forward bias voltage of 0.45 V in the present work. This value of $\Delta\Phi_\mathrm{imf}$ is much lower than the observed barrier height lowering of 126 meV (Fig. 2). Therefore, the image-force lowering alone cannot account for the lowering of the barrier height.

The decrease in the barrier height and the increase in the ideality factor with a decrease in the operating temperature is indicative of a deviation from the pure thermionic emission theory and possibly the thermionic-field-emission (TFE) mechanism warrants consideration. The parameter that determines the relative importance of the TE, TFE and field emission (FE) is given by [22].

$$E_{00} = h/4\pi\left(N_\mathrm{D}/m_\mathrm{e}^*\varepsilon_\mathrm{s}\right) = 18.5 \times 10^{-15}\left(N_\mathrm{D}/m_\mathrm{r}^*\varepsilon_\mathrm{r}\right) 1/2\,\mathrm{eV} \qquad (5)$$

In the case of our diode, with $N_\mathrm{D} = 2.5 \times 10^{21}\,\mathrm{m}^{-3}$, $m_\mathrm{e}^* = 0.067 m_\mathrm{e}$ and $\varepsilon_\mathrm{r} = 12.8$, this value turns out to be 1.056 meV. According to the theory TFE dominates only when $E_{00} \approx kT$ and the value of E_{00} calculated from (6) is less than kT by a factor of six, even at 77 K. The barrier-height lowering accounting for the TFE and using the theoretically calculated value of E_{00} is given by [23].

$$\Delta\Phi_\mathrm{TFE} = (3/2)^{2/3}(E_{00})^{2/3} V_\mathrm{d}^{1/3}, \qquad (6)$$

where V_d is the built-in potential.

For the E_{00} value of 1.056 meV and a V_d of 0.91 V this value is 13.3 meV, which again cannot account for the observed barrier-height lowering.

2.1.3 Barrier-height inhomogenity. More recently it has been proposed that the barrier height has a lateral Gaussian distribution with a mean barrier height [5]. The reduction in the barrier height with temperature has been explained by the lateral distribution of the barrier height. The assumption of the Gaussian distribution of the barrier height yields the following equation for the barrier height.

$$\Phi_\mathrm{b} = \Phi_\mathrm{bmean} - \sigma_\mathrm{S}^2/\,(2kT/q)\,, \qquad (7)$$

where Φ_b is the zero-bias barrier height, Φ_bmean is the mean barrier height, and σ_S is the standard deviation of the barrier distribution.

The mean barrier height is the same as the barrier height measured by capacitance measurements. Capacitance measurements yield a barrier height which is essentially at zero electric field. Since the flat-band barrier height is also obtained at zero electric field, both the quantities are the same [18]. Using this relation and $\Phi_\mathrm{b}^\mathrm{f} = \Phi_\mathrm{bmean}$, a value of $\sigma_\mathrm{S} = 53.3$ meV and $\Phi_\mathrm{b} = 1.012$ eV were obtained. Using these values in (7), a continuous curve was generated as a function of the operating temperature, which is plotted in Fig. 2. It can be observed from the figure that although the curve obtained by using (7) agrees well with the values of the zero-bias barrier height in the 77–210 K range, it deviates appreciably from the experimental points at higher temperatures.

Another approach to the lateral inhomogenities in the Schottky barrier heights was proposed by Sullivan et al. [13] and Tung [14]. They proposed that the Schottky barrier consists of laterally inhomogenous patches of different barrier heights. The patches with lower barrier height have a larger ideality factor and vice versa. Schmitsdorf et al. [15] found a linear correlation between the zero-bias barrier height and the ideality factors using Tung's theoretical approach. The extrapolation of the linear fit to the these data yields the homogeneous barrier height at an ideality factor of 1.01. A similar analysis of our data to this effect is presented in Fig. 4.

It is observed that the barrier height correlates linearly with the ideality factors measured at temperatures below 200 K. The homogeneous barrier height determined from this analysis yields a value of 0.97 eV.

2.1.4 The ideality factor and T_0 effect. The variation in the ideality factor with temperature is shown in Fig. 2, and is

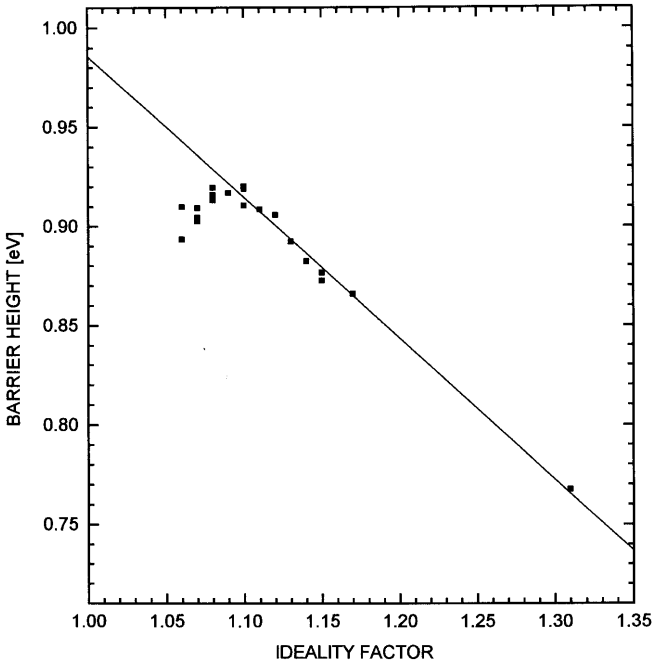

Fig. 4. The variation of the zero-bias barrier height with temperature. The *continuous curve* is calculated using (7) with $\sigma_0 = 53.3$ meV. The *continuous curve* matches well with the points in the 77–210 K range and shows considerable deviation at higher temperatures

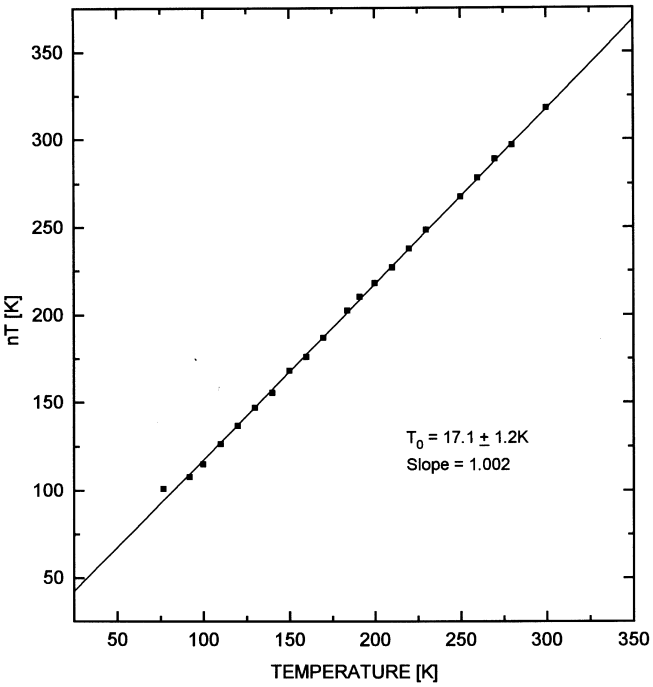

Fig. 5. Plot shows nT vs. T. The linear behaviour of the experimental values is determined by (8). The value of the slope and the T_0 are shown in the figure

called the T_0 effect [1]. The ideality factor of the diodes showing this behaviour varies with temperature as

$$n = 1 + T_0/T \,, \tag{8}$$

where T_0 is a constant.

This implies that a plot of nT vs. T is a straight line with a slope of unity and the intercept T_0 at the ordinate. Figure 5 shows such a plot with the slope equal to 1.002, which is close to unity as predicted by the empirical relation and the intercept $T_0 = 17.1 \pm 1.2$ K. The value of T_0 can vary between 10–100 K for diodes on the same slice of GaAs [2]. The T_0 effect could be due to generation recombination current in the depletion region or due to the TFE. The *C–V* characteristics of the diode under study at different frequencies in the range of 1 kHz–1 MHz were independent of the frequency within this range. This indicates that the diode does not contain a measurable amount of deep levels within the space-charge region and therefore the influence of the minority carriers on current transport can be neglected [24, 25].

2.1.5 Effect of image force. The possibility of the image-force lowering influencing the observed variation of the ideality factor was checked using the relation [21].

$$[n_{\mathrm{imf}}]^{-1} = 1 - 1/4 \left(q^3 N_{\mathrm{D}}/8\pi^2 \varepsilon_{\mathrm{s}}^3\right)^{1/4} \times (\Phi_{\mathrm{b}} - V - \Phi_{\mathrm{n}} - kT/q)^{-3/4} \,. \tag{9}$$

This equation yields a value of 1.011 at a typical bias value of 0.45 V at 300 K and a value of 1.008 at a temperature of 77 K. This shows that the image-force lowering cannot account for the observed variation in the ideality factor.

2.1.6 Effect of thermionic field emission. The ideality factor is further analyzed by considering the variation in the ideality factor n caused by a tunnelling current. The relation for the variation in the ideality factor is given by [22].

$$n = qE_{00}/kT \coth\left(qE_{00}/kT\right) \,, \tag{10a}$$

$$n = qE_0/kT \,, \tag{10b}$$

where

$$E_0 = E_{00} \coth\left(qE_{00}/kT\right) \,. \tag{10c}$$

Figure 6 shows a plot of E_0 vs. kT/q. The intercept on the E_0 axis of such a plot yields the value of E_{00} for the Schottky diode under study. It can be seen from the figure that the experimental points are linear with temperature up to the kT value corresponding to the temperature of 92 K. A careful examination of the plot reveals a slight curvature near 77 K. This can be confirmed only by determining the ideality factors from the *I–V* characteristics recorded below this temperature. Since our experimental setup is limited to an operating temperature of 77 K, this could not be confirmed. If it is assumed that the curvature near 77 K is indeed present, then it reveals a higher characteristic energy, which cannot be explained by the above theories. In order to confirm the higher value of the characteristic energy, another method was used which requires plotting of the theoretically determined values of n vs. temperature on a $1/n$ vs. $1000/T$ plot [26]. The following relation was used to generate such theoretical plots with E_{00} as the parameter.

$$1/n = kT/q\left[E_0/\left(1-\beta\right)\right] \,, \tag{11}$$

where β indicates the bias dependence of the barrier height.

Since the values of $1/n$ are sensitive to changes near unity such a plot provides a good check to determine whether the

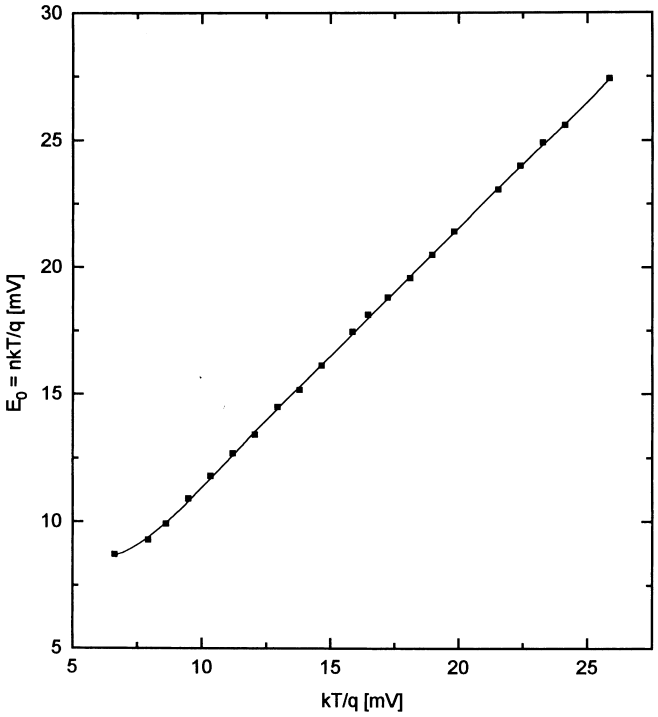

Fig. 6. Plot of E_0 vs. T using (10c) assuming TFE. The slight curvature near 92 K indicates the possibility of a higher characteristic energy than is predicted by the theory and estimated using (5)

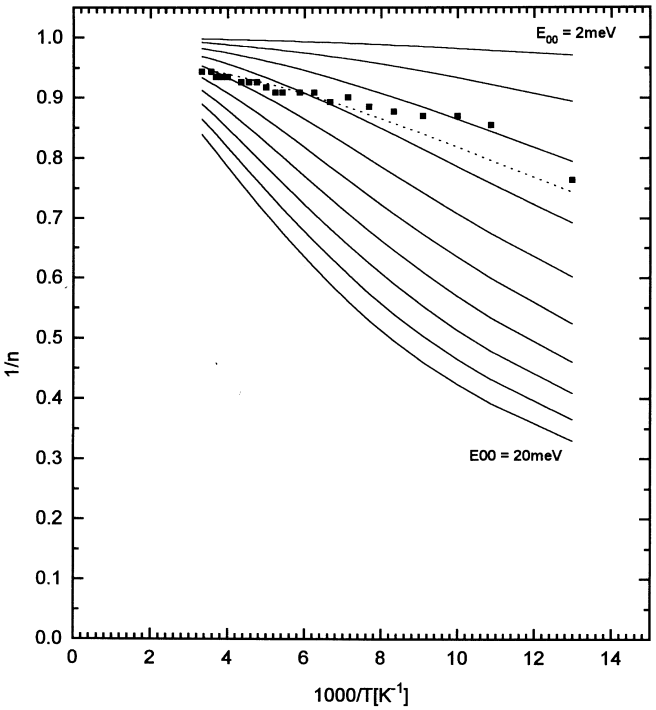

Fig. 7. Plot showing $1/n$ vs. $1/T$ curves (*solid lines*) with E_{00} as the parameter ranging from 2–20 meV in steps of 2 meV generated using (11) and $\beta = 0$. The *experimental points* are also superimposed on the theoretically generated plot. The *dotted line* shown on the plot represents a *curve* with the value of $E_{00} = 6.5$ meV and $\beta = 0.032$

dominating mechanism is TE or TFE. The experimentally determined values of the ideality factor are superimposed on such a plot to determine the values of E_{00} and β approximately. Figure 7 shows such a plot. It can be observed that the experimental points match closely to the curve with $E_{00} = 6.5$ meV and $\beta = 0.032$. Therefore, the diode under test certainly exhibits high characteristic energies not expected for the doping concentration range used in our GaAs film, implying a conduction mechanism dominated by TFE.

2.1.7 Influence of barrier height inhomogenity. Using the potential fluctuations model [5], the ideality factor is given by the relation

$$1/n = 1 - \gamma + \sigma_s q\zeta/kT\,. \tag{12}$$

Using the experimentally determined values of n at different temperatures and the value of σ_0 obtained from (7), the values of $\gamma = 0.006$ and $\zeta = 0.0236$ were obtained. The experimentally determined values and the continuous curve representing a fit to these values using the parameters obtained by using (12) are shown in Fig. 2.

2.1.8 Richardson constant. The Richardson constant is usually determined from the intercept of $\ln(J_s/T^2)$ vs. $1000/T$ plot. Figure 8a shows the plot obtained by the usual method. This plot yields a Richardson constant of $0.32\,\mathrm{A\,cm^{-2}K^{-2}}$ and a Φ_b of 0.85 eV. The value of the Richardson constant is about one order magnitude lower compared to the theoretical value of $3\,\mathrm{A\,cm^{-2}K^{-2}}$ [27]. A careful observation of the experimental points shows that the points up to a temperature of 160 K exhibit a better linearity. A best fit to the points in the 160–300 K range yields an A^{**} value of $43.2\,\mathrm{A\,cm^{-2}K^{-2}}$

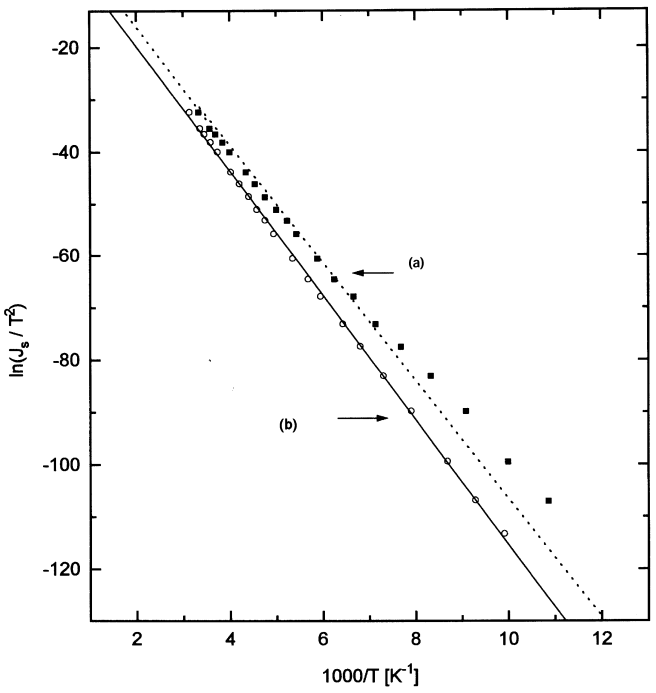

Fig. 8. The activation energy plots of (a) $\ln(J_s/T^2)$ vs. $1000/T$ and (b) $\ln(J_s/T^2)$ vs. $1000/nT$. The values using (a) show deviation from linearity below the operating temperature of 160 K. The values of A^{**} and the barrier height, Φ_b using (a) and (b) are $A^{**} = 43.2\,\mathrm{A\,cm^{-2}K^{-2}}$, $\Phi_b = 0.94$ eV using a linear fit to the values in the 160–300 K range and $A^{**} = 64.7\,\mathrm{A\,cm^{-2}K^{-2}}$, $\Phi_b = 1.02$ eV, respectively

and a Φ_b value of 0.94 eV. For the case in which the ideality factor is a strong function of the temperature, a modified Richardson plot has been proposed which uses a plot of $\ln(J_s/T^2)$ vs. $1/n(T)T$ [3]. Figure 8b also shows such a plot of $\ln(J_s/T^2)$ vs. $1/n(T)T$. The values of A^{**} and the barrier height determined from this plot are 64.7 A cm^{-2}K^{-2} and 1.02 eV, respectively. The values determined from the usual method in the temperature range of 160–300 K and by using the modified Richardson plot are much higher than the theoretical value of 3 A cm^{-2}K^{-2}. The higher values have been explained in terms of the variation of the barrier height with temperature [27–29]. In such a case the zero-axis intercept of the Richardson plot yields

$$A^{**}_{\text{observed}} = A^{**} \exp\left[-q/k\left(\mathrm{d}\Phi_b^f/\mathrm{d}T\right)\right] \tag{13}$$

and the slope gives the barrier height. Hence the value of A^{**} obtained from the Richardson plot needs to be corrected to obtain the actual value of A^{**}. The corrected value of A^{**} is related to the observed value of the Richardson constant by the relation

$$A^{**}_{\text{corrected}} = A^{**}_{\text{observed}} \exp\left[q/k\left(\mathrm{d}\Phi_b^f/\mathrm{d}T\right)\right], \tag{14}$$

where Φ_b^f is the flat-band barrier height.

The $A^{**}_{\text{corrected}}$ as determined from the observed value obtained from the modified Richardson plot is 0.27 A cm^{-2}K^{-2}. The lower value of this constant can be explained by the presence of an interfacial layer between the semiconductor and the metal [30]. The process of Schottky diode fabrication consisted of etching the oxide on the semiconductor surface by HCl prior to the Schottky metal deposition. But it is possible that an oxide layer could have formed during the time of loading the samples into the metallization chamber. The Richardson constant in the presence of such an interfacial layer is given by the relation [30]

$$A^{**}_{\text{oxide}} = A^{**} \exp\left(-0.26\chi^{0.5}\delta\right), \tag{15}$$

where χ is the mean barrier height of the oxide–semiconductor interface in eV, δ is the thickness of the interfacial layer in Å.

A value of 0.08 eV for the mean barrier height has been used to explain the observed behaviour in the case of MIS structures on GaAs [11]. But values in the range of 0.08–0.14 eV have been used for different interfacial layer thickness to calculate the value of A^{**}_{oxide} [27]. Our value of 0.27 A cm^{-2}K^{-2} indicates an interfacial layer of 30 Å between the metal and the semiconductor and a value of 0.095 eV for the mean barrier height of the oxide–semiconductor interface.

3 Discussion

The variation of the zero-bias barrier height with temperature exhibits two different trends in the temperature ranges of 77–150 K and 150–300 K. The decreasing barrier height with decreasing temperature has been reported for various Schottky diodes [3–7]. The variation in the zero-bias barrier height in the range 160–300 K is similar to the variation in the barrier height determined by *C–V* measurements. The behaviour of the flat-band barrier height, calculated from the *J–V* characteristics, in the 150–300 K range, is similar. The slope of the flat-band barrier height vs. temperature correlates well with earlier reports of the variation in the barrier height assuming that it is entirely dependent on the energy band gap alone. The possibility of an inhomogeneous barrier distribution correlates well for the values of the zero-bias barrier height below 210 K but shows considerable deviation at higher temperatures (Fig. 2). It can also be observed (Fig. 2) that the increase in the ideality factor with decreasing temperature is more pronounced below 150 K. The usual Richardson plot, assuming the transport to be dominated by TE, yields a value 43.2 A cm^{-2}K^{-2}, which is in the range of values obtained by other workers [1, 28] only if the temperature range of 160–300 K is used. Although the characteristic energy E_{00}, calculated using (5) for the present case turns out to be much lower, the plot of E_0 vs. T and the comparison of the experimental values of the ideality factor with the theoretically estimated values using (11) indicate the possibility of a high characteristic energy. All these results indicate the possibility of the onset of TFE-dominated current below 160 K.

The possible origin of such high characteristic energies implies that the conduction mechanism is dominated by TFE at low temperatures instead of TE. The origin of high characteristic energies was not predicted by the simple theory, but has been related to several effects. The parameter, E_{00} is related to the transmission probability of the carrier through the barrier. It is affected by the electric field at the semiconductor surface and the density of states at the semiconductor surface. Any mechanism such as the geometrical inhomogeneities arising due to crystal defects, the surface roughness and the device periphery, local pile up of dopants, the presence of a relatively thick insulator interfacial layer with low dielectric constant, and the charge in the interfacial layer could possibly increase the electric field near the semiconductor surface [6]. Multistep tunnelling through the interface states also yield high characteristic apparent energies [12]. In our case the value of the Richardson constant obtained after correction can be justified by considering an interfacial oxide layer of 30 Å. Although the presence of an oxide layer could not be confirmed in the present study, this approach does offer a plausible explanation for the electric field enhancement and the possible origin of high characteristic energies. Sullivan et al. [13] and Tung [14] have explained the observed effects on the barrier height and the ideality factor by considering lateral inhomogenities in the Schottky barrier height. Their approach assumes an unchanging Richardson constant and attributes the experimental observations to the lateral inhomogenity only. It is very likely that this could be the reason for the observed anomalies since the formation of metal–semiconductor interfaces involves some form of defects and result in an inhomogenous Schottky barrier height.

4 Conclusions

Forward-bias *I–V* characteristics of a Au/n-GaAs Schottky diode were measured in the temperature range of 77–300 K. Although the doping concentration of the n-GaAs epi-layer was well within the domain of the TE as predicted by the theory, anomalies were observed with respect to the ideality factor and the zero-bias barrier height as a function of operating temperature. The observations cannot be explained from

the viewpoint of pure TE theory alone and were attributed to the possibility of TFE-dominated current transport. This possibility was further supported by the observed high characteristic energy in the current transport. The flat-band barrier height, which is the real fundamental quantity, was found to decrease with the increase in the operating temperature in the range of 150–300 K. This dependence of the flat-band barrier height follows that of the energy band gap, where it decreases with increasing temperature. The values of the barrier height determined by different methods are almost consistent. The value of the Richardson constant after applying the appropriate corrections was found to be $0.27\,\mathrm{A\,cm^{-2}K^{-2}}$. The lower value of the Richardson constant can be explained in terms of the possible presence of an interfacial oxide layer of 30 Å between the metal and the semiconductor. The interfacial oxide could also be the possible reason for an enhancement in the electric field at the surface of the semiconductor leading to the observed high characteristic energies and current transport dominated by thermionic field emission.

Acknowledgements. This work has been carried out as part of the joint research programme between Bharat Electronics Ltd., Bangalore and the Indian Institute of Science, on MOCVD.

References

1. F.A. Padovani, G.G. Sumner: J. Appl. Phys. **36**, 3744 (1965)
2. F.A. Padovani: In *Semiconductors and Semimetals*, Vol. 6, ed. by R.K. Willardson, A.C. Beer (Academic Press, New York 1971)
3. R. Hackam, P. Harrop: IEEE Trans. Electron Devices **19**, 1231 (1972)
4. A.S. Bhuiyan, A. Martinez, D. Esteve: Thin Solid Films **161**, 93 (1988)
5. J.H. Werner, H.H. Guttler: J. Appl. Phys. **69**, 1522 (1991)
6. Zs.J. Horvath: Mater. Res. Soc. Symp. Proc. **260**, 359 (1992)
7. S. Chand, J. Kumar: Appl. Phys. A **63**, 171 (1996)
8. J.D. Levine: J. Appl. Phys. **42**, 3991 (1971)
9. C.R. Crowell: Solid State Electron. **20**, 171 (1977)
10. C.R. Crowell, V.L. Rideout: Solid State Electron. **12**, 89 (1969)
11. S. Ashok, J.M. Borrego, R. Gutmann: Solid State Electron. **22**, 621 (1979)
12. P.L. Hanselaer, W.H. Laflere, R.L. Van Meirhaege, F. Cardon: J. Appl. Phys. **56**, 2309 (1984)
13. J.P. Sullivan, R.T. Tung, M.R. Pinto, W.R. Graham: J. Appl. Phys. **70**, 7403 (1991)
14. R.T. Tung: Phys. Rev. B **45**, 13 509 (1992)
15. R.F. Schmitsdorf, T.U. Kampen, W. Mönch: J. Vac. Sci. Technol. B **15**, 1221 (1997)
16. M.K. Hudait, P. Modak, S. Hardikar, S.B. Krupanidhi: Solid State Commun. **103**, 411 (1997)
17. S.M. Sze: *Physics of Semiconductor Devices*, 2nd edn. (Wiley, New York 1981)
18. L.F. Wagner, R.W. Young, A. Sugerman: IEEE Electron. Devices Lett. **4**, 320 (1983)
19. M.B. Panish, H.C. Casey: J. Appl. Phys. **40**, 1663 (1969)
20. F. Oswald: Z. Naturforsch. A **10A**, 927 (1955)
21. M. Wittmer: Phys. Rev. B **42**, 5249 (1990)
22. F.A. Padovani, R. Stratton: Solid State Electron. **9**, 695 (1966)
23. E.H. Rhoderick, R.H. Williams: *Metal-Semiconductor contacts*, 2nd edn. (Clarendon, Oxford 1988)
24. J.H. Werner, K. Ploog, H.J. Queisser: Phys. Rev. Lett. **57**, 1080 (1986)
25. J.H. Werner: In *Metallization and Metal-Semiconductor Interfaces*, ed. by I.P. Batra (Plenum, New York 1989) p. 325
26. Zs.J. Horvath: Proc. Of the Int. Conference on Advanced Semiconductor Devices and Microsystems, Warsaw, Poland (1996) p. 263
27. A.K. Srivastava, B.M. Arora, S. Guha: Solid State Electron. **24**, 185 (1981)
28. M. Borrego, R.J. Gutmann, S. Ashok: Appl. Phys. Lett. **30**, 1669 (1977)
29. Yu.A. Gol'dberg, E.A. Posse, B.V. Tsarenkov: Sov. Phys. Semicond. **9**, 337 (1975)
30. H.C. Card, E.H. Rhoderick: J. Phys. D **4**, 1589 (1971)